Prediction of critical heat flux on surface under boiling in case of IVR-ERVC by using CFD simulation

IOP Conf. Series: Materials Science and Engineering **576** (2019) 012042 doi:10.1088/1757-899X/576/1/012042

Prediction of critical heat flux on surface under boiling in case of IVR-ERVC by using CFD simulation

Rasool Urfa[1], Daogang Lu[1], Noor Farooq Asran[2], Ansari Munib[1] and Rasool Aazim[1]

Beijing Key Laboratory of Passive Safety Technology for Nuclear Energy,
[1]North China Electric Power University, Beijing 102206, China,
[1]Pakistan Institute of Engineering and Applied Sciences.

E-mail: urfarasool@ncepu.edu.cn

Abstract. The efficacy of in-vessel through external reactor vessel cooling (IVR-ERVC) is strongly correlated with the critical heat flux (CHF) on the lower head of reactor pressure vessel (RPV). The high limit of CHF prevents the RPV from failure by extracting much heat out of the vessel through the circulation of working fluid in external flow channel. In present study, the deionized water is allowed to flow through curved flow channel having radius of curvature of 368mm and hydraulic diameter of 40mm with square cross-section. The heat flux of 1500kWm^{-2} is applied perpendicular to the convex wall of the channel. The CHF on the wall of flow channel has been predicted by incorporating CFD based two-phase (liquid-vapor) boiling model. The investigations on spatial variation of pressure, temperature, and velocity and heat flux acquired as a result of numerical simulations have been discussed in detail. The CHF and average HTC is predicted as 1.798e+04kWm^{-2} and 38.981kWm^{-2}K^{-1} respectively.

1. Introduction

The researchers have proposed after Three Mile Island accidents, that a pressure vessel can enhance ample heat transfer when submerged in the coolant to retrofit in-vessel retention of melting core. IVR-ERVC is considered as a requisite strategy for banishing utmost heat out of the RPV by introducing external flow channel outside of the RPV. The coolant while flowing through the ERVC extracts heat out of the pressure vessel and keeps its temperature low[1-3]. The CHF is the maximum limit which is bearable by the vessel. As far as the CHF on the outer surface of the vessel under boiling remains higher than the wall heat flux from the melting core, the temperature of outer vessel could be retained near saturation temperature of water in order to maintain the integrity of RPV. It is therefore, necessary to predict the CHF limit on the outer surface of vessel in order to do necessary measures for its enhancement and for the enhancement of boiling heat transfer.

Many experimental and theoretical studies on the enhancement of boiling heat transfer have been conducted in literature [4-8]. Presently, the broadly used CFD approach in engineering technologies for the simulation of two-phase flows with profound amount of void fraction was the Eulerian approach[9]. In this model, the conservation of mass, momentum and energy of both vapor and liquid phase had been considered separately and weighted by the volume fraction which depicted the assembled mean probability of the inhabitation for each phase at a particular point with respect to time and space. The sink and the source are the interchange terms between phases in the conservation

equations. These referents comprised of empirical or analytical correlations, depicting the interfacial forces, mass flux and the heat flux as a function of mean flow aspects. The mass and momentum transfer between two phases were analyzed by the bubble dynamics up to the moderate level of void fraction. The characteristics bubble diameter was used in order to consider deformation. The turbulence intensity in the flow channel and near the walls was strongly affected by the bubble dynamics at high Reynolds number. In case of diabatic boiling flows, when the heat was transferred from heated wall to the bulk fluid at high rates due to the generation and departure of vapor bubbles, the source term illustrating the mechanics of those phenomena at heated wall cannot be neglected.

In this paper, the two-phase boiling flow in case of IVR-ERVC has been studied by CFD simulation. Moreover, the elaborated discussion referring to the spatial distribution of heat flux, velocity, temperature and pressure has also been proposed, along with the prediction on CHF of IVR-ERVC by incorporating CFD vapor-liquid boiling model.

2. Mathematical modelling for CFD

There are several different mechanisms in which heat is transferred from hot body to the surrounding fluid i.e. in boiling. At the part of the heating surface where no bubble inhabits, the heat flows to the subcooled liquid directly like a single-phase flow. The part of the heating surface where the generation of vapors occurs at the nucleation sites extracts heat out of the surface. With the escaping of bubbles, the liquid mixing mechanism exists. The cold liquid from the bulk comes into contact with the heating surface as a result of recirculation around the detaching bubble, this phenomenon conducts additional cooling. In terms of two sets of conservation equations, governing the balance of mass, momentum, and energy of each phase the two-phase subcooled boiling model has been established. In governing equations, the interaction terms couple the interface transfer of mass, momentum, and energy. The water-liquid is taken as continuous phase whereas water-vapor is illustrated as a dispersed or secondary phase.

Conservation of mass,

$$\nabla.(\rho_m u_m) = 0 \tag{1}$$

Mass average velocity (u_m),

$$u_m = \sum_{k=1}^{2} \frac{\alpha_k \rho_k u_k}{\rho_m} \tag{2}$$

Mixture density (ρ_m),

$$\rho_m = \sum_{k=1}^{2} \alpha_k \rho_k \tag{3}$$

Conservation of momentum(p)[10],

$$\nabla.(\rho_m u_m u_m) = -\nabla p + \nabla[\mu_m(\nabla u_m + \nabla u_m^T)] + \rho_m g + \nabla(\sum_{k=1}^{2} \alpha_k \rho_k u_{dr,k} u_{dr,k}) \tag{4}$$

The viscosity of mixture (μ_m),

$$\mu_m = \sum_{k=1}^{2} \alpha_k \mu_k \tag{5}$$

The drift velocity ($u_{dr,k}$) for k-phase,

$$u_{dr,k} = u_k - u_m \tag{6}$$

The slip velocity (u_{vl}),

$$u_{vl} = u_v - u_l \tag{7}$$

The drift velocity is correlated with the slip velocity as follow,

$$u_{dr,k} = u_{vl} - \sum_{k=1}^{2} \frac{\alpha_k \rho_k}{\rho_m} u_{lk} \tag{8}$$

The relative velocity consisting of diffusion term as a result of dispersion by the turbulent [11]:

$$u_{vl} = \frac{(\rho_v - \rho_m) d_v^2 a}{18 \mu_{leff} f_{drag}} - \frac{v_{t,m}}{\alpha_v \sigma_D} \nabla \alpha_l \tag{9}$$

Where $v_{t,m}$ is the turbulent viscosity of mixthe ture, σ_D , is the Prandtl dispersion coefficient. The drag force f_{drag} , is considered as[12]:

$$f_{drag} = \begin{cases} 1 + 0.15 Re_v^{0.687} & Re_v \leq 1000 \\ 0.0183 Re_v & Re_v > 1000 \end{cases} \tag{10}$$

The Reynolds number,

$$Re_v = \frac{u_m d_v}{v_m} \tag{11}$$

The acceleration (a),

$$a = g - (u_m \nabla) u_m \tag{12}$$

The energy equation for the mixture is as follows;

$$\nabla . \sum_{k=1}^{2} (\alpha_k u_k \rho_k h_k) = \nabla . \left(k_{eff} \nabla T \right) + Q_w \tag{13}$$

$$k_{eff} = \left[\sum_{k=1}^{2} \alpha_k (k_k + k_t) \right] \tag{14}$$

The effective conductivity (k_{eff}) and the turbulent thermal conductivity (k_t) are related as;

$$k_t = \frac{C_P \mu_t}{Pr_t} \tag{15}$$

The heat source i.e. the wall heat flux $Q_w$which is equivalent to the latent heat required for phase change. C_P is specific heat capacity.By incorporating continuity equation for the phases, the void fraction for dispersed phase i.e. vapors is computed as;

$$\nabla . (\alpha_v \rho_v v_m) = -\nabla . \left(\alpha_v \rho_v v_{dr,v} \right) + \sum_{k=1}^{2} (m_{lv} - m_{vl}) \tag{16}$$

'm', is the mass transfer through evaporation and condensation. The turbulence model (k-ε) has been used in this investigation due to complex modeling in the multiphase simulation. It is mainly effectual for turbulent core flows. The equations for turbulent kinetic energy and dissipation rate are represented as;

$$\nabla . (\rho_m u_m k) = \nabla . \left(\frac{\mu_{t,m} \nabla k}{\sigma_k} \right) + G_{k,m} - \rho_m \epsilon \tag{17}$$

$$\nabla . (\rho_m u_m \epsilon) = \nabla . \left(\frac{\mu_{t,m} \nabla \epsilon}{\sigma_\epsilon} \right) - C_2 \rho_m \frac{\epsilon}{k} (C_{1\epsilon} G_{k,m} - C_{2\epsilon} \rho_m \epsilon) \tag{18}$$

The turbulent viscosity and turbulent kinetic viscosity are taken as[13];

$$\mu_{t,m} = C_\mu \rho_m \frac{k^2}{\epsilon} \tag{19}$$

$$G_{k,m} = \mu_{t,m} (\nabla u_m + \nabla u_m^T) : \nabla u_m \tag{20}$$

σ_k, σ_ϵ, $C_{1\epsilon}$, $C_{2\epsilon}$, C_μ equal to 1, 1.3, 1.44, 1.92, 0.09 respectively are the empirical constants[14].The effective viscosity is given as;

$$\mu_{eff} = \mu_{leff} + \mu_{t,m} \tag{21}$$

The wall heat flux (Q_w) is constituted into three parts:

$$Q_w = Q_c + Q_e + Q_q \tag{22}$$

The first part is convective heat flux (Q_c):

$$Q_c = A_1 St \rho_l C_{pl} u_l (T_w - T_l);\ A_1 = 1 - A_2 \tag{23}$$

Where $A_1$and A_2 are the fraction of the wall surface under the influence of liquid and vapor formed on the wall surface respectively. T_l , and u_l are the liquid temperature and velocity at the cell closed to the wall. St is the Stanton number.

$$S_t = \frac{Nu}{Re_l Pr_l} \tag{24}$$

The active nucleation density is correlated as;

$$n = [210(T_w - T_{sat})]^{1.805} \tag{25}$$

The second part is evaporation heat flux (Q_e) for the generation of vapor bubbles:

$$Q_e = nf\left(\frac{\pi d_{BW}^3}{6}\right)\rho_v h_{vl} \tag{26}$$

The bubble frequency (f) is driven from the correlation:

$$f = \sqrt{\frac{4g(\rho_{leff} - \rho_v)}{3d_{BW}\rho_{leff}}} \tag{27}$$

As depicted that the frequency is dependent on bubble diameter and phase density. The average of multiple sizes of bubbles is usually considered as a single size bubble in literature. The bubble departure diameter is computed as:

$$d_{BW} = \min\left[1.4, 0.6.\exp\left(-\frac{\Delta T_{sub}}{45}\right)\right] \tag{28}$$

The third part is quenching heat flux (Q_q) representing heat flux from heating wall to the bulk liquid by departing or collapsing bubbles during the bubble eruption cycle. The Q_q is calculated from the temperature difference of wall and the bulk liquid multiplied by the heat transfer coefficient. Whereas, K=2[15]

$$Q_q = \left(\frac{2}{\pi}\sqrt{k_{leff}\rho_{leff}C_{pleff}f}\right)A_2(T_w - T_l) \quad ` \tag{29}$$

$$A_2 = nK\left(\frac{\pi d_{BW}^2}{4}\right) \tag{30}$$

By accounting the mass transfer from the liquid to the vapor phase on the heating wall is:

$$m_{wv} = \frac{Q_e}{h_{vl} + C_{pleff}(T_{sat} - T_l)} \tag{31}$$

The mass transfer rate from liquid to the vapor (evaporation) and from vapor to the liquid (condensation) inside the fluid is evaluated by using the following equations:

$$m_{lv} = \begin{cases} \frac{r_{lv}\alpha_l\rho_{leff}(T_l - T_{sat})}{T_{sat}}; T_l \geq T_{sat} \\ 0 \qquad\qquad\qquad ; T_l < T_{sat} \end{cases} \tag{32}$$

$$m_{vl} = \begin{cases} \frac{r_{vl}\alpha_v\rho_{veff}(T_{sat} - T_l)}{T_{sat}}; T_v \geq T_{sat} \\ 0 \qquad\qquad\qquad ; T_v < T_{sat} \end{cases} \tag{33}$$

Phase volume fraction is represented as α, density is ρ whereas r_{lv} and $r_{vl}$are mass transfer time parameters with unit ms^{-1}[16]. The aforementioned boiling model is coupled with the CFD simulation where the wall boundary condition is the wall heat flux taken as $1500kWm^{-2}$ and the reservoir temperature is considered as 20˚C and 80˚C. By considering the velocity, void fraction and heating wall temperature distribution under sub cooling effect, the heat transfer from the heating wall to the flowing fluid is examined, CHF and the HTC are predicted.

3. Numerical simulation

For the numerical simulation of CFD, the discretization of the governing equations has been done by considering second order upwind scheme. The SIMPLE (semi-implicit method for pressure linked equations) algorithm is adopted for the coupling of pressure and velocity. The k-Ɛ model is used for modeling turbulence in flow boiling. The illustration of geometric parameters of curved flow channel with downward facing heating wall and the boundary conditions are summarized in Table-1.

Table 1. Specifications of curved channel and boundary conditions

Outlet gauge pressure, P_2	21.16	[kPa]
Inlet velocity, v_l	0.347	[ms^{-1}]
Inlet temperature, T_i	293	[K]
Heat flux, Q	1500	[kWm^{-2}]
Volumetric flow rate,	6.626	[m^3s^{-1}]
Hydraulic diameter, d_h	0.040	[m]
Bend angle of channel, θ	90˚	[degrees]
Radius of curvature	0.368	[m]

The fluid is allowed to flow from the inlet at the bottom of the channel to the outlet on the top of the channel. The inlet boundary condition is set with a fluid velocity of 0.347ms^{-1}, and temperature of 293K whereas the outlet boundary condition is set at a pressure of 21.61kPa. The supplied heat flux to the convex wall of the channel is 1500kWm^{-2}. The concave wall of the channel is kept as adiabatic due to insulation effect.

4. Results and discussions

4.1. Variation of pressure field

Figure.1 depicts non uniform pressure distribution of water coolant through curved flow channel from inlet to the outlet under constant heating through its convex wall. The static pressure observed to be decreased from 7.75E5Pa to 1.36E4Pa while flowing upward along flow field. The pressure gradient through curved channel is plotted in Figure.2. It can be seen in plot that from inlet to the outlet of the channel the pressure initially dropped because of the utilization of energy for the generation of secondary phase (vapors) but after reaching a certain point i.e. nearby 0.13m, the pressure gradient suddenly raised due to increasing interactions between two phases with the continuous formation of vapor phase under boiling.

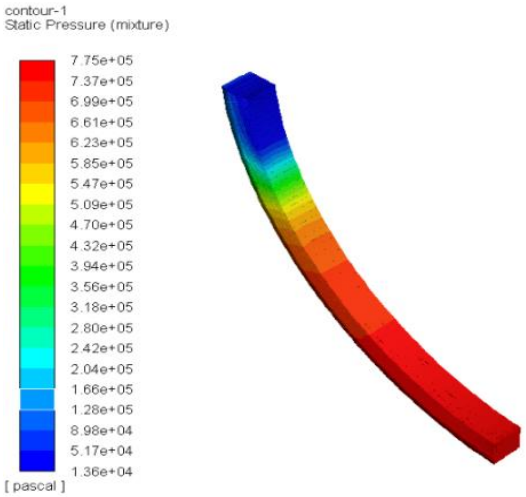

Figure 1. Pressure distribution

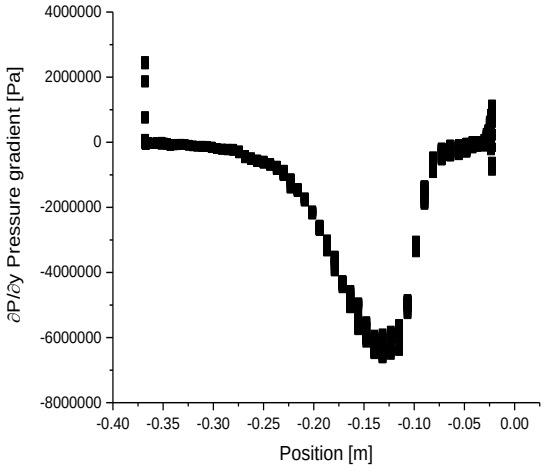

Figure 2. Pressure gradient

4.2. Variation of temperature field

Figure. 3 shows distribution of temperature on heated wall of the channel. It varied from 293K to 20200K all the way from inlet to the outlet. The generation and accumulation of vapors on heated surface at consistent heat flux supplied perpendicular to the convex wall formed vapor blanket near outlet of the channel which consequently increased wall temperature due to low thermal conductivity of vapor phase. The distribution of void fraction on heated wall is plotted against position in Figure.4. The void fraction can be seen concentrated from 0.20m to 0.10m due to the occurance of large number of vapors which could not extract heat out of the heated wall and acquired temperature upto 20200K.

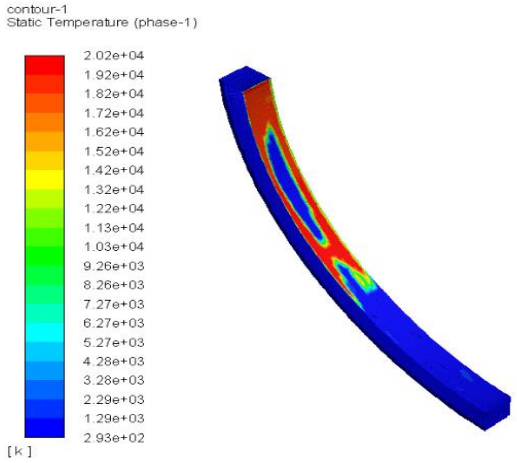

Figure 3. Temperature distribution

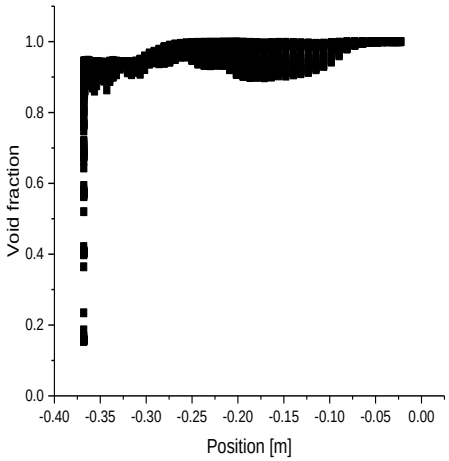

Figure 4. Void fraction distribution on heated wall

4.3. Variation of velocity field

The variation of fluid velocity is illustrated in Figure. 5. It can be seen in the figure that the flow rate in the premises of heated wall of the channel is considerably higher than the premises of adiabatic wall due high energy and upward slip velocity of vapors as compared to liquid phase. The buoyancy effect kept vapors to stay near upper heated wall in a wide range.

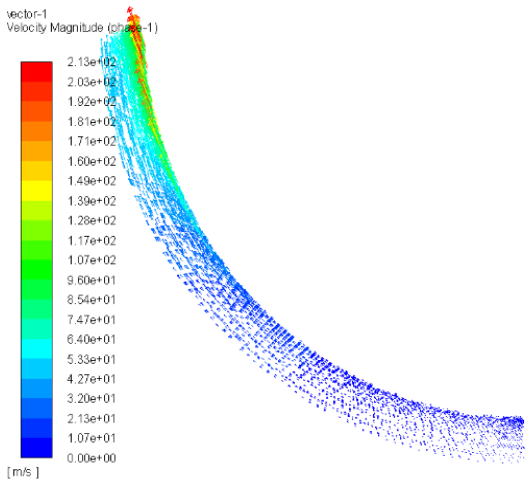

Figure 5.Velocity distribution

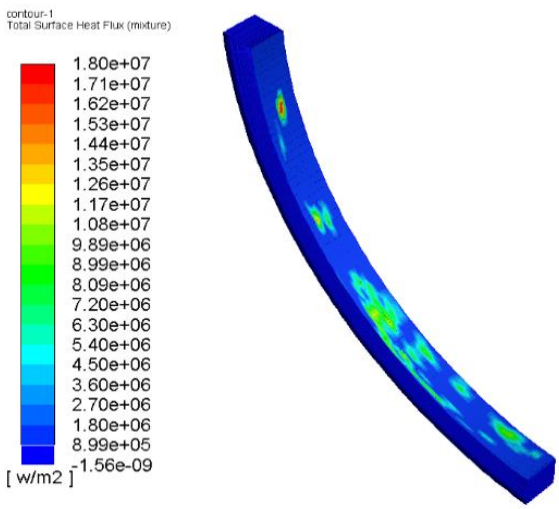

Figure 6. Heat flux distribution

4.4. The prediction of CHF

The distribution of heat flux on heated wall of the curved channel is illustrated in Figure.6. The continuous supply of heat flux increased formation of vapors, after a certain limit the accumulation of vapors created vapor blanket and entrapped heat within the channel by blocking liquid pathways and rewetting. As a result, dry spots started to originate on heated surface which then extended into dry patches thus, wall temperature increased abruptly. The increased rate of vapor formation induced thermal resistance and wall stresses which brought boiling to the transition regime followed by the turbulent regime and gradually to the utmost limit of bearable heat flux i.e. critical heat flux. The critical heat flux (CHF) on heated surface in present case is calculated as 1.798e+04kWm^{-2} near outlet of the channel whereas, the average heat transfer coefficient (HTC) is calculated as 38.981kWm^{-2}K^{-1}.

5. Conclusions

A two-phase CFD boiling model has been used to numerically investigate the flow boiling characteristics of water coolant flowing through the external curved flow channel by considering temperature dependent quantities and in the turbulent flow regime. It has been concluded that the pressure gradient initially decreases from inlet to the outlet of the channel due to the utilization of energy in the formation of secondary phase then after reaching a certain limit the pressure gradient started to increase with increasing interaction of vapor and liquid phase. The flow velocity appeared greater near the heating wall than that of adiabatic wall due to the effect of boiling. Under the influence of buoyancy, the vapors accumulated on the upper heating wall of the channel, incorporated thermal resistance augmented the wall temperature because of low thermal conductivity of vapor phase and eventually the boiling crises occurred which can be seen initiated near the outlet of the channel. The CHF and average HTC is predicted as 1.798e+04kWm^{-2} and 38.981kWm^{-2}K^{-1} respectively.

6. Abbreviations

The following abbreviations are used in this manuscript:

ρ	*Density [kgm^{-3}]*	C_p	*Specific heat [Jkg^{-1}K^{-1}]*
u	*Velocity [ms^{-1}]*	m	*Inter-phase mass transfer*
α	*Volume fraction of liquid or vapor phase*	$k-\epsilon$	*Turbulence dissipation rate - turbulence kinetic energy [Jkg^{-1}]*
μ	*Kinematic viscosity [m^{2}s^{-1}]*	Nu	*Nusselt number*
v	*Dynamic viscosity [Pas]*	Pr	*Prandtl number*
u_{dr}	*Drift velocity [ms^{-1}]*	St	*Stanton number*
u_{vl}	*Slip velocity [ms^{-1}]*	Re	*Reynolds number*
σ	*Surface tension [Nm^{-1}]*	n	*Nucleation site density [m^{-2}]*
f_{drag}	*Drag force [N]*	r	*Mass transfer time[s^{-1}]*
d	*Diameter[m]*	Q_w	*Wall heat flux [Wm^{-2}]*
a	*Acceleration [ms^{-2}]*	Q_e	*Heat flux due to evaporative [Wm^{-2}]*
g	*Gravity [ms^{-2}]*	Q_c	*Heat flux due to convection [Wm^{-2}]*
h	*Enthalpy [Jkg^{-1}]*	Q_q	*Heat flux due to quenching [Wm^{-2}]*
k	*Thermal conductivity [Wm^{-1}K^{-1}]*	A_s	*Surface area [m^2]*
α	*Volume fraction of vapor or liquid*	A_1	*Area fraction of wall under the influence of liquid [m^2]*
T	*Temperature [K]*	A_2	*Area fraction of wall under the influence of vapor [m^2]*
ΔT	*Sub cooled [K]*	f	*Bubble departure frequency[s^{-1}]*
Q	*Heat flux [Wm^{-2}]*	d_{BW}	*Bubble departure diameter[m]*

$\dot{Q}$	*Heat transfer rate [kW]*	h_{vl}	*Latent heat of vaporization [Jkg^{-1}]*
G	*Mass flux [kgm^{-2}s^{-1}]*	V	*Voltage [V]*
P_1	*Inlet pressure of channel [Pa]*	I	*Current [A]*
P_2	*Outlet pressure of the channel [Pa]*	θ	*Bend angle of the channel [degree]*

Subscripts

v	*Vapor*	t	*Turbulent*
l	*Liquid*	b	*Bulk*
m	*Mixture*	dr	*Drift*
k	*Summation index*	e	*Evaporation*
sat	*Saturated*	c	*Convection*
eff	*Effective*	q	*Quenching*

7. References

[1] Rempe, J.L., et al., *In-vessel retention-recent efforts and future needs*. 2004: Idaho National Laboratory.
[2] Rempe, J.L., et al., *Insights from investigations of in-vessel retention for high powered reactors*. 2005: Idaho National Laboratory.
[3] Rempe, J.L., et al., *In-vessel retention strategy for high power reactors.* Final Report, Idaho National Engineering and Environmental Laboratory, Report No. INEEL/EXT-04-02561, 2003.
[4] Henry, R.E. and H.K. Fauske, *External cooling of a reactor vessel under severe accident conditions.* Nuclear Engineering and Design, 1993. **139**(1): p. 31-43.
[5] Chu, T.Y., et al., *Ex-vessel boiling experiments: laboratory-and reactor-scale testing of the flooded cavity concept for in-vessel core retention Part I: Observation of quenching of downward-facing surfaces.* Nuclear Engineering and Design, 1997. **169**(1-3): p. 77-88.
[6] Chu, T.Y., et al., *Ex-vessel boiling experiments: laboratory-and reactor-scale testing of the flooded cavity concept for in-vessel core retention Part II: Reactor-scale boiling experiments of the flooded cavity concept for in-vessel core retention.* Nuclear Engineering and Design, 1997. **169**(1-3): p. 89-99.
[7] Theofanous, T.G. and S. Syri, *The coolability limits of a reactor pressure vessel lower head.* Nuclear Engineering and Design, 1997. **169**(1-3): p. 59-76.
[8] Theofanous, T.G., et al., *Quantification of Limits to Coolability in ULPU-2000 Configuration IV*. CRSS-02.05, 2002. **3**.
[9] Drew, D.A. and S.L. Passman, *Theory of multicomponent fluids*. Vol. 135. 2006: Springer Science & Business Media.
[10] Fluent, A., *Ansys fluent theory guide.* ANSYS Inc., USA. **15317**: p. 724-746.
[11] Manninen, M., V. Taivassalo, and S. Kallio, *On the mixture model for multiphase flow*. 1996, Technical Research Centre of Finland Finland.
[12] Schiller, L., *A drag coefficient correlation.* Zeit. Ver. Deutsch. Ing., 1933. **77**: p. 318-320.
[13] Lucas, D., E. Krepper, and H.M. Prasser, *Use of models for lift, wall and turbulent dispersion forces acting on bubbles for poly-disperse flows.* Chemical Engineering Science, 2007. **62**(15): p. 4146-4157.
[14] Launder, B.E. and D.B. Spalding, *The numerical computation of turbulent flows*, in *Numerical Prediction of Flow, Heat Transfer, Turbulence and Combustion*. 1983, Elsevier. p. 96-116.
[15] Kenning, D.B.R., *Fully-developed nucleate boiling: overlap of areas of influence and interference between bubble sites.* International Journal of Heat and Mass Transfer, 1981. **24**(6): p. 1025-1032.
[16] Abedini, E., et al., *Numerical investigation of subcooled flow boiling of a nanofluid.* International Journal of Thermal Sciences. **64**: p. 232-239.